Capacitance of Microstrip Lines with Inhomogeneous Substrate

Jean-Fu Kiang, *Member, IEEE*

Abstract— **A mode-matching approach combined with Galerkin's method is proposed in this paper to calculate the capacitance matrix of microstrip lines embedded in an inhomogeneous stratified medium. Eigenmodes in each layer is first solved numerically, and the potential in each layer can be expressed in terms of these eigenmodes. Coupling between two sets of eigenmodes in contiguous layers are described by defining reflection matrices. A Green's function is thus obtained in terms of these eigenmode sets to relate the potential to a line charge. Integral equation is then constructed relating the charge distribution and the imposed voltage on the microstrip surface. Galerkin's method is next applied to solve the charge distribution and hence the capacitance matrix. Several inhomogeneous profiles are studied to understand the effects of inhomogeneities on the capacitance and relevant parameters.**

I. INTRODUCTION

FOR a microstrip deposited at the interafce between a dielectric and free space, approximate closed form for capacitance is plausible [1]. Conformal mapping technique has been applied to calculate the capacitance matrix of several microstrips lying in the same plane enclosed by a rectangular conducting box [2].

For several microstrip lines emdedded in different layers of a stratified medium, numerical methods are often resorted. In [3]–[5], a spatial domain approach using the free space Green's function has been developed to calculate the capacitance and the inductance matrices of multiconductor transmission lines located arbitrarily in a multilayered medium of finite extent. The potential in the medium is expressed in terms of the free charge at the conductor-dielectric interfaces and the total charge at the dielectric-dielectric interfaces.

Variational method in the spectral domain has been used to calculate the capacitance matrix of microstrips in an laterally open structure [6], [7]. Perfect conductor planes can also be put aside the whole layered structure to facilitate the analysis, and the Green's function within side walls are expressed in terms of sinusoidal functions with discrete wave numbers [8], [9].

Each dielectric layer is assumed homogeneous in the spectral domain analysis. However, some practical substrate materials contain inhomogeneities. For example, glass fibers are implanted within an epoxy circuit board to enhance its mechanical strength [10]. In [11], two microstrips are built on a substrate with finite extent. A notch is cut in the substrate amidst two microstrips to reduce their coupling. The dielectric constant underneath the microstrip can also be increased locally to focus the power guided by the strip [12]. In such cases, conventional spectral domain methods do not apply, and the spatial domain approaches may render too many unknowns to model the equivalent surface charge especially when the dielectric constant is a continuous function of coordinates.

In this paper, we will derive an integral equation in the spectral domain with discrete wave numbers. The kernel is constructed based on the eigenmodes in each inhomogeneous layer, which are solved numerically for arbitrary permitivity profile.

Manuscript received November 10, 1995; revised June 14, 1996. This work was supported by the National Science Council, Taiwan, ROC under Contract NSC85-2213-E005-010.

The author is with the Department of Electrical Engineering, National Chung-Hsing University, Taichung, Taiwan, ROC.

Publisher Item Identifier S 0018-9480(96)06906-2.

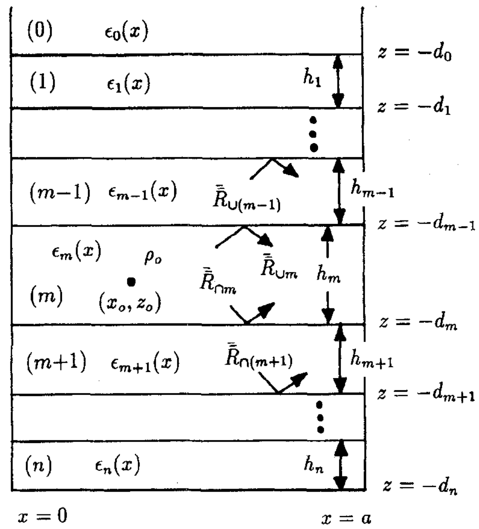

Fig. 1. Geometrical configuration of a line charge embedded in layer (m) of a stratified inhomogeneous medium.

II. FORMULATION

In Fig. 1, we show the configuration of a line charge source in layer (m) of a stratified medium. The whole structure is uniform in the y direction. In each layer, the dielectric constant is a piecewise continuous function of x and is independent of z. Two perfect electric conductor walls are located at $x=0$ and $x=a$ as the potential reference.

In the electroquasi-static (EQS) limit [13], potential in layer (m) in the absence of charge source is obtained by solving the following Laplace's equation

$$\left(\epsilon_m^{-1}(x)\frac{\partial}{\partial x}\epsilon_m(x)\frac{\partial}{\partial x}+\frac{\partial^2}{\partial z^2}\right)\phi(x,z)=0. \tag{1}$$

0018–9480/96$05.00 © 1996 IEEE

By separation of variables, $\phi(x,z)$ can be expressed as a product of $\psi(x)\eta(z)$, and (1) is reduced to

$$\begin{aligned}\epsilon_m^{-1}(x)\frac{d}{dx}\epsilon_m(x)\frac{d}{dx}\psi(x) &= -k^2\psi(x)\\ \frac{d^2}{dz^2}\eta(z) &= k^2\eta(z)\end{aligned} \quad (2)$$

Next, choose a set of basis functions $S_p(x)=\sqrt{2/a}\sin(\alpha_p x)$ with $\alpha_p = p\pi/a$. These basis functions have orthonormal properties that $\langle S_q(x), S_p(x)\rangle = \delta_{qp}$ where the inner product is defined over the interval $[0,a]$. Expand the nth eigensolution $\psi_n(x)$ by these basis functions as $\psi_n(x)=\sum_{p=1}^N b_{np}S_p(x)$, and substitute it into (2). Take the inner product of $S_q(x)$ with the resulting equation and apply the orthonormality property of $S_p(x)$'s to obtain

$$\sum_{p=1}^{N}\langle S_q'(x), \epsilon_m(x)S_p'(x)\rangle b_{np} = k_n^2\sum_{p=1}^{N}\langle S_q(x), \epsilon_m(x)S_p(x)\rangle b_{np}, \quad 1\le q\le N. \quad (3)$$

From (3), N eigenvalues k_n^2 and their associated eigenvectors $\bar{b}_n$ can be obtained. These eigensolutions are normalized to have

$$\langle \psi_r(x), \epsilon_m(x)\psi_s(x)\rangle = \bar{b}_r^t\cdot \bar{\bar{C}}_m\cdot \bar{b}_s \quad (4)$$

where the (q,p)th element of $\bar{\bar{C}}_m$ is $\langle S_q(x), \epsilon_m(x)S_p(x)\rangle$.

Next, consider a line charge with density ρ_0 located at (x_0, z_0) in layer (m) of the stratified medium. In the absence of other layers, the potential is obtained by solving the Poisson's equation

$$\left(\epsilon_m^{-1}(x)\frac{\partial}{\partial x}\epsilon_m(x)\frac{\partial}{\partial x}+\frac{\partial^2}{\partial z^2}\right)\phi(x,z) = -\frac{\rho_0}{\epsilon_m(x_0)}\delta(x-x_0)\delta(z-z_0). \quad (5)$$

The solution $\phi(x,z)$ can be expressed in terms of the eigensolutions $\psi_p(x)$ as

$$\begin{aligned}\phi(x,z) &= \sum_{p=1}^{N}\frac{\rho_0}{2k_p}\psi_p(x)\psi_p(x_0)e^{-k_p|z-z_0|}\\ &= \frac{\rho_0}{2}\bar{\psi}_m^t(x)\cdot \bar{\bar{K}}_m^{-1}\cdot e^{-\bar{\bar{K}}_m|z-z_0|}\cdot\bar{\psi}_m(x_0)\end{aligned} \quad (6)$$

where $\bar{\bar{K}}_m = \mathrm{diag}\cdot[k_1,k_2,\ldots,k_N]$, $e^{-\bar{\bar{K}}_m|z-z_0|} = \mathrm{diag}\cdot[e^{-k_1|z-z_0|}, e^{-k_2|z-z_0|},\ldots,e^{-k_N|z-z_0|}]$, and $\bar{\psi}_m^t(x) = [\psi_1(x),\psi_2(x),\ldots,\psi_N(x)]$ are eigensolutions in layer (m).

In the presence of other inhomogeneous layers as in Fig. 1, the potential in layer (m) can be expressed as

$$\begin{aligned}\phi_m(x,z) = \bar{\psi}_m^t(x) &\cdot\left[e^{-\bar{\bar{K}}_m z_m}\cdot\bar{A}_m + e^{\bar{\bar{K}}_m z_m}\cdot\bar{B}_m\right.\\ &\left.+\frac{\rho_0}{2}\bar{\bar{K}}_m^{-1}\cdot e^{-\bar{\bar{K}}_m|z_m-z_m'|}\cdot\bar{\psi}_m(x_0)\right]\end{aligned} \quad (7)$$

where $z_m = z+d_m$ and $z_m' = z_0+d_m$. The first term in the bracket decays in the positive z direction, and the second term decays in the negative z direction. At $z=-d_m$, define a reflection matrix $\bar{\bar{R}}_{\cap m}$ which relates the upward-decaying potential to the downward-decaying potential as

$$\bar{A}_m = \bar{\bar{R}}_{\cap m}\cdot\left[\bar{B}_m + \frac{\rho_0}{2}\bar{\bar{K}}_m^{-1}\cdot e^{-\bar{\bar{K}}_m z_m'}\cdot\bar{\psi}_m(x_0)\right]. \quad (8)$$

Similarly, define another reflection matrix $\bar{\bar{R}}_{\cup m}$ at $z=-d_{m-1}$ as

$$\begin{aligned}e^{\bar{\bar{K}}_m h_m}\cdot\bar{B}_m = \bar{\bar{R}}_{\cup m}&\cdot\left[e^{-\bar{\bar{K}}_m h_m}\cdot\bar{A}_m+\frac{\rho_0}{2}\bar{\bar{K}}_m^{-1}\right.\\ &\left.\cdot e^{-\bar{\bar{K}}_m(h_m-z_m')}\cdot\bar{\psi}_m(x_0)\right].\end{aligned} \quad (9)$$

From (8) and (9), $\bar{A}_m$ and $\bar{B}_m$ are solved explicitly as

$$\begin{aligned}\bar{A}_m &= \frac{\rho_0}{2}\left[\bar{\bar{I}}-\bar{\bar{R}}_{\cap m}\cdot e^{-\bar{\bar{K}}_m h_m}\cdot\bar{\bar{R}}_{\cup m}\cdot e^{-\bar{\bar{K}}_m h_m}\right]^{-1}\\ &\quad\cdot\bar{\bar{R}}_{\cap m}\cdot\left[e^{-\bar{\bar{K}}_m h_m}\cdot\bar{\bar{R}}_{\cup m}\cdot\bar{\bar{K}}_m^{-1}\cdot e^{-\bar{\bar{K}}_m(h_m-z_m')}\right.\\ &\quad\left.+\bar{\bar{K}}_m^{-1}\cdot e^{-\bar{\bar{K}}_m z_m'}\right]\cdot\bar{\psi}_m(x_0)\\ \bar{B}_m &= \frac{\rho_0}{2}\left[\bar{\bar{I}}-e^{-\bar{\bar{K}}_m h_m}\cdot\bar{\bar{R}}_{\cup m}\cdot e^{-\bar{\bar{K}}_m h_m}\cdot\bar{\bar{R}}_{\cap m}\right]^{-1}\\ &\quad\cdot e^{-\bar{\bar{K}}_m h_m}\cdot\bar{\bar{R}}_{\cup m}\cdot\left[e^{-\bar{\bar{K}}_m h_m}\cdot\bar{\bar{R}}_{\cap m}\cdot\bar{\bar{K}}_m^{-1}\cdot e^{-\bar{\bar{K}}_m z_m'}\right.\\ &\quad\left.+\bar{\bar{K}}_m^{-1}\cdot e^{-\bar{\bar{K}}_m(h_m-z_m')}\right]\cdot\bar{\psi}_m(x_0).\end{aligned} \quad (10)$$

The potential in layer (m) can thus be written in a compact form as

$$\phi_m(x,z) = \rho_0\bar{\psi}_m^t(x)\cdot\bar{\bar{T}}_{mm}(z_m,z_m')\cdot\bar{\psi}_m(x_0) \quad (11)$$

where

$$\begin{aligned}\bar{\bar{T}}_{mm}(z_m,z_m') &= \frac{1}{2}\Big\{e^{-\bar{\bar{K}}_m z_m}\cdot\left[\bar{\bar{I}}-\bar{\bar{R}}_{\cap m}\cdot e^{-\bar{\bar{K}}_m h_m}\cdot\bar{\bar{R}}_{\cup m}\cdot e^{-\bar{\bar{K}}_m h_m}\right]^{-1}\\ &\quad\cdot\bar{\bar{R}}_{\cap m}\cdot\left[e^{-\bar{\bar{K}}_m h_m}\cdot\bar{\bar{R}}_{\cup m}\cdot\bar{\bar{K}}_m^{-1}\cdot e^{-\bar{\bar{K}}_m(h_m-z_m')}\right.\\ &\quad\left.+\bar{\bar{K}}_m^{-1}\cdot e^{-\bar{\bar{K}}_m z_m'}\right]+e^{-\bar{\bar{K}}_m(h_m-z_m)}\\ &\quad\cdot\left[\bar{\bar{I}}-\bar{\bar{R}}_{\cup m}\cdot e^{-\bar{\bar{K}}_m h_m}\cdot\bar{\bar{R}}_{\cap m}\cdot e^{-\bar{\bar{K}}_m h_m}\right]^{-1}\cdot\bar{\bar{R}}_{\cup m}\\ &\quad\cdot\left[e^{-\bar{\bar{K}}_m h_m}\cdot\bar{\bar{R}}_{\cap m}\cdot\bar{\bar{K}}_m^{-1}\cdot e^{-\bar{\bar{K}}_m z_m'}\right.\\ &\quad\left.+\bar{\bar{K}}_m^{-1}\cdot e^{-\bar{\bar{K}}_m(h_m-z_m')}\right]+\bar{\bar{K}}_m^{-1}\cdot e^{-\bar{\bar{K}}_m|z_m-z_m'|}\Big\}.\end{aligned} \quad (12)$$

The potential in layer (l) with $l<m$ can be expressed as

$$\phi_l(x,z) = \bar{\psi}_l^t(x)\cdot\left[e^{-\bar{\bar{K}}_l z_l}+e^{-\bar{\bar{K}}_l(h_l-z_l)}\cdot\bar{\bar{R}}_{\cup l}\cdot e^{-\bar{\bar{K}}_l h_l}\right]\cdot\bar{A}_l. \quad (13)$$

Imposing the boundary condition that potential is continuous at $z=-d_{m-1}$, we have

$$\begin{aligned}\bar{\psi}_{m-1}^t(x)\cdot\Big[\bar{\bar{I}}&+e^{-\bar{\bar{K}}_{m-1}h_{m-1}}\\ &\cdot\bar{\bar{R}}_{\cup(m-1)}\cdot e^{-\bar{\bar{K}}_{m-1}h_{m-1}}\Big]\cdot\bar{A}_{m-1}\\ &= \rho_0\bar{\psi}_m^t(x)\cdot\bar{\bar{T}}_{mm}(h_m,z_m')\cdot\bar{\psi}_m(x_0).\end{aligned} \quad (14)$$

Take the inner product of $\epsilon_{m-1}(x)\bar{\psi}_{m-1}(x)$ with (14) to obtain

$$\bar{A}_{m-1} = \rho_0\Big[\,\overline{\overline{I}} + e^{-\overline{\overline{K}}_{m-1}h_{m-1}} \cdot \overline{\overline{R}}_{\cup(m-1)} \cdot e^{-\overline{\overline{K}}_{m-1}h_{m-1}}\Big]^{-1} \cdot \overline{\overline{H}}_{(m-1)m} \cdot \overline{\overline{T}}_{mm}\,(h_m, z_m') \cdot \bar{\psi}_m(x_0) \quad (15)$$

where $\overline{\overline{H}}_{qp} = \langle\bar{\psi}_q(x), \epsilon_q(x)\bar{\psi}_p^t(x)\rangle$. Imposing the boundary condition that the potential and the normal electric flux density are continuous at $z = -d_l$, we have

$$\bar{\psi}_l^t(x) \cdot \Big[\,\overline{\overline{I}} + e^{-\overline{\overline{K}}_l h_l} \cdot \overline{\overline{R}}_{\cup l} \cdot e^{-\overline{\overline{K}}_l h_l}\Big] \cdot \bar{A}_l = \bar{\psi}_{l+1}^t(x) \cdot \Big[\,\overline{\overline{I}} + \overline{\overline{R}}_{\cup(l+1)}\Big] \cdot e^{-\overline{\overline{K}}_{l+1}h_{l+1}} \cdot \bar{A}_{l+1} \quad (16)$$

$$\epsilon_l(x)\bar{\psi}_l^t(x) \cdot \overline{\overline{K}}_l \cdot \Big[\,\overline{\overline{I}} - e^{-\overline{\overline{K}}_l h_l} \cdot \overline{\overline{R}}_{\cup l} \cdot e^{-\overline{\overline{K}}_l h_l}\Big] \cdot \bar{A}_l = \epsilon_{l+1}(x)\bar{\psi}_{l+1}^t(x) \cdot \overline{\overline{K}}_{l+1} \cdot \Big[\,\overline{\overline{I}} - \overline{\overline{R}}_{\cup(l+1)}\Big] \cdot e^{-\overline{\overline{K}}_{l+1}h_{l+1}} \cdot \bar{A}_{l+1}. \quad (17)$$

Take the inner product of $\epsilon_l(x)\bar{\psi}_l(x)$ with (16) to have

$$\bar{A}_l = \Big[\,\overline{\overline{I}} + e^{-\overline{\overline{K}}_l h_l} \cdot \overline{\overline{R}}_{\cup l} \cdot e^{-\overline{\overline{K}}_l h_l}\Big]^{-1} \cdot \overline{\overline{H}}_{l(l+1)} \cdot \Big[\,\overline{\overline{I}} + \overline{\overline{R}}_{\cup(l+1)}\Big] \cdot e^{-\overline{\overline{K}}_{l+1}h_{l+1}} \cdot \bar{A}_{l+1}. \quad (18)$$

Take the inner product of $\psi_l(x)$ with (17) to have

$$\overline{\overline{K}}_l \cdot \Big[\,\overline{\overline{I}} - e^{-\overline{\overline{K}}_l h_l} \cdot \overline{\overline{R}}_{\cup l} \cdot e^{-\overline{\overline{K}}_l h_l}\Big] \cdot \bar{A}_l = \overline{\overline{H}}{}^t_{(l+1)l} \cdot \overline{\overline{K}}_{l+1} \cdot \Big[\,\overline{\overline{I}} - \overline{\overline{R}}_{\cup(l+1)}\Big] \cdot e^{-\overline{\overline{K}}_{l+1}h_{l+1}} \cdot \bar{A}_{l+1}. \quad (19)$$

From (18) and (19), we obtain the recursive relation between the reflection matrices as

$$\begin{aligned}\overline{\overline{R}}_{\cup(l+1)} = &\Big\{\Big[\,\overline{\overline{I}} - e^{-\overline{\overline{K}}_l h_l} \cdot \overline{\overline{R}}_{\cup l} \cdot e^{-\overline{\overline{K}}_l h_l}\Big]^{-1} \cdot \overline{\overline{K}}{}_l^{-1} \cdot \overline{\overline{H}}{}^t_{(l+1)l} \cdot \overline{\overline{K}}_{l+1} \\ &+ \Big[\,\overline{\overline{I}} + e^{-\overline{\overline{K}}_l h_l} \cdot \overline{\overline{R}}_{\cup l} \cdot e^{-\overline{\overline{K}}_l h_l}\Big]^{-1} \cdot \overline{\overline{H}}_{l(l+1)}\Big\}^{-1} \\ &\cdot \Big\{\Big[\,\overline{\overline{I}} - e^{-\overline{\overline{K}}_l h_l} \cdot \overline{\overline{R}}_{\cup l} \cdot e^{-\overline{\overline{K}}_l h_l}\Big]^{-1} \cdot \overline{\overline{K}}{}_l^{-1} \cdot \overline{\overline{H}}{}^t_{(l+1)l} \cdot \overline{\overline{K}}_{l+1} \\ &- \Big[\,\overline{\overline{I}} + e^{-\overline{\overline{K}}_l h_l} \cdot \overline{\overline{R}}_{\cup l} \cdot e^{-\overline{\overline{K}}_l h_l}\Big]^{-1} \cdot \overline{\overline{H}}_{l(l+1)}\Big\}. \end{aligned} \quad (20)$$

Similarly, the potential in layer (l) with $l > m$ can be expressed as

$$\phi_l(x,z) = \bar{\psi}_l^t(x) \cdot \Big[e^{-\overline{\overline{K}}_l z_l} \cdot \overline{\overline{R}}_{\cap l} + e^{\overline{\overline{K}}_l z_l}\Big] \cdot \bar{B}_l. \quad (21)$$

Imposing the boundary condition that potential is continuous at $z = -d_m$, we have

$$\bar{B}_{m+1} = \rho_0\Big[e^{-\overline{\overline{K}}_{m+1}h_{m+1}} \cdot \overline{\overline{R}}_{\cap(m+1)} + e^{\overline{\overline{K}}_{m+1}h_{m+1}}\Big]^{-1} \cdot \overline{\overline{H}}_{(m+1)m} \cdot \overline{\overline{T}}_{mm}\,(0, z_m') \cdot \bar{\psi}_m(x_0). \quad (22)$$

Imposing the boundary condition that the potential and the normal electric flux density are continuous at $z = -d_l$, we obtain the recursive relation between the reflection matrices as

$$\begin{aligned}\overline{\overline{R}}_{\cap l} = &\Big\{\Big[\,\overline{\overline{I}} - e^{-\overline{\overline{K}}_{l+1}h_{l+1}} \cdot \overline{\overline{R}}_{\cap(l+1)} \cdot e^{-\overline{\overline{K}}_{l+1}h_{l+1}}\Big]^{-1} \cdot \overline{\overline{K}}{}_{l+1}^{-1} \cdot \Big(\overline{\overline{H}}{}^t_{(l+1)l}\Big)^{-1} \cdot \overline{\overline{K}}_l \\ &+ \Big[\,\overline{\overline{I}} + e^{-\overline{\overline{K}}_{l+1}h_{l+1}} \cdot \overline{\overline{R}}_{\cap(l+1)} \cdot e^{-\overline{\overline{K}}_{l+1}h_{l+1}}\Big]^{-1} \cdot \overline{\overline{H}}{}_{l(l+1)}^{-1}\Big\}^{-1} \\ &\cdot \Big\{\Big[\,\overline{\overline{I}} - e^{-\overline{\overline{K}}_{l+1}h_{l+1}} \cdot \overline{\overline{R}}_{\cap(l+1)} \cdot e^{-\overline{\overline{K}}_{l+1}h_{l+1}}\Big]^{-1} \cdot \overline{\overline{K}}{}_{l+1}^{-1} \cdot \Big(\overline{\overline{H}}{}^t_{(l+1)l}\Big)^{-1} \cdot \overline{\overline{K}}_l \\ &- \Big[\,\overline{\overline{I}} + e^{-\overline{\overline{K}}_{l+1}h_{l+1}} \cdot \overline{\overline{R}}_{\cap(l+1)} \cdot e^{-\overline{\overline{K}}_{l+1}h_{l+1}}\Big]^{-1} \cdot \overline{\overline{H}}{}_{l(l+1)}^{-1}\Big\}. \end{aligned} \quad (23)$$

Consider a microstrip line embedded in layer (m) with a specific voltage applied on the strip surface, then the potential distribution in layer (m) can be expressed in terms of the surface charge density $\rho(x)$ as

$$\phi_m(x,z) = \bar{\psi}_m^t(x) \cdot \overline{\overline{T}}_{mm}\,(z_m, z_m') \cdot \int_{x_1}^{x_2} dx'\rho(x')\bar{\psi}_m(x'). \quad (24)$$

The potential on the strip surface is equal to the applied voltage. Thus, an integral equation is obtained

$$\bar{\psi}_m^t(x) \cdot \overline{\overline{T}}_{mm}\,(z_m', z_m') \cdot \int_{x_1}^{x_2} dx'\rho(x')\bar{\psi}_m(x') = V, \quad x_1 \le x \le x_2. \quad (25)$$

To solve (25), we first choose a set of basis functions to represent the charge density distribution as

$$\rho(x') = \sum_{p=1}^{P} \alpha_p f_p(x') \quad (26)$$

where $f_p(x')$'s are linear local basis functions. Substituting (26) into (25) and using the same set of basis functions as the weighting functions, the following matrix equation is obtained

$$\sum_{p=1}^{P} \langle f_q(x), \bar{\psi}_m^t(x)\rangle \cdot \overline{\overline{T}}_{mm}\,(z_m', z_m') \cdot \langle f_p(x'), \bar{\psi}_m(x')\rangle\alpha_p = V\int_{x_1}^{x_2} dx f_q(x), \qquad 1 \le q \le P. \quad (27)$$

The capacitance matrix of microstrip lines is then derived from the charge distribution.

III. Numerical Results

In Fig. 2, the effective dielectric constant of a microstrip line is shown as a function of the relative permittivity of the substrate under the inhomogeneous layer. The results agree reasonably with those in [12].

Next, two periodical substrate structures similar to that in [10] is modeled. In Fig. 3, the capacitance of the microstrip

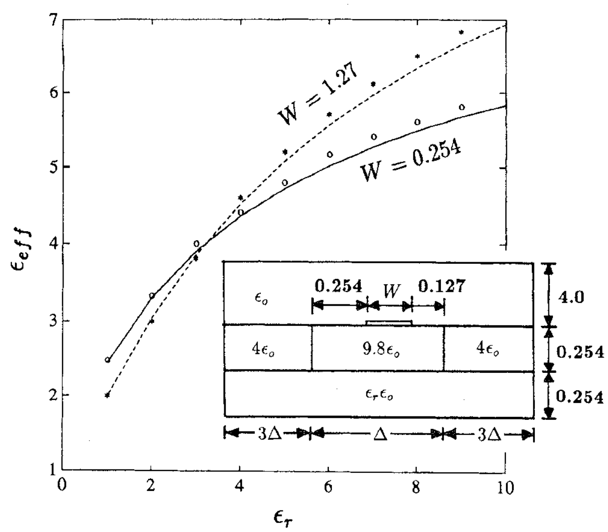

Fig. 2. Effective dielectric constant of a microstrip line affected by the permittivity of the lowest substrate layer, o and *: results from [12].

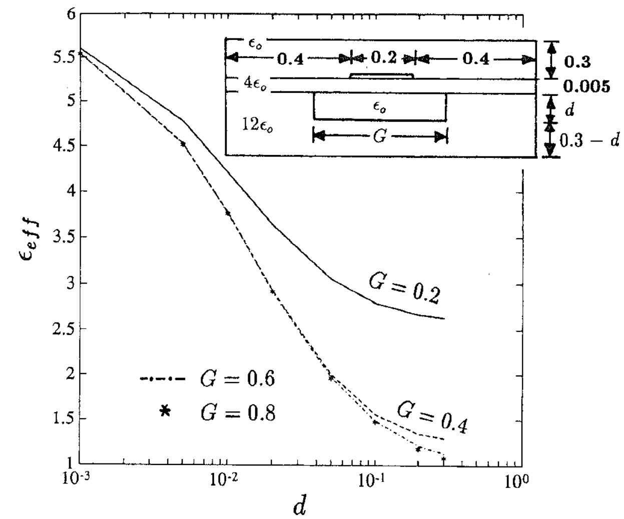

Fig. 4. Effective dielectric constant affected by the air pocket underneath the microstrip line.

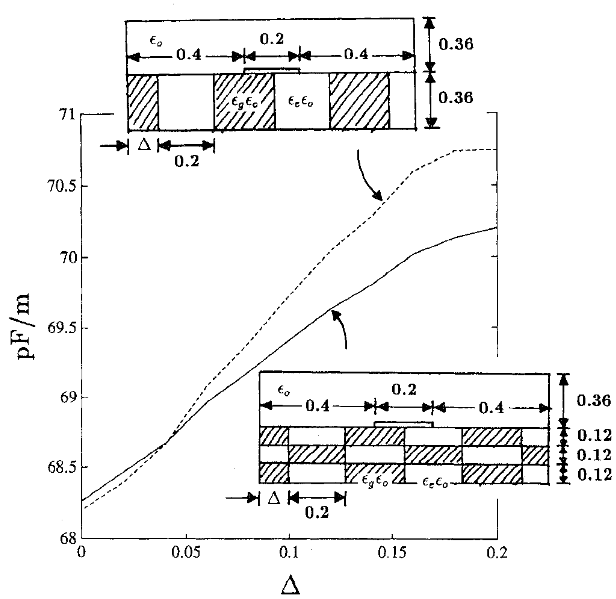

Fig. 3. Capacitance variation as the periodical substrate is laterally shifted, $\epsilon_g = 5.5$, $\epsilon_e = 3.6$.

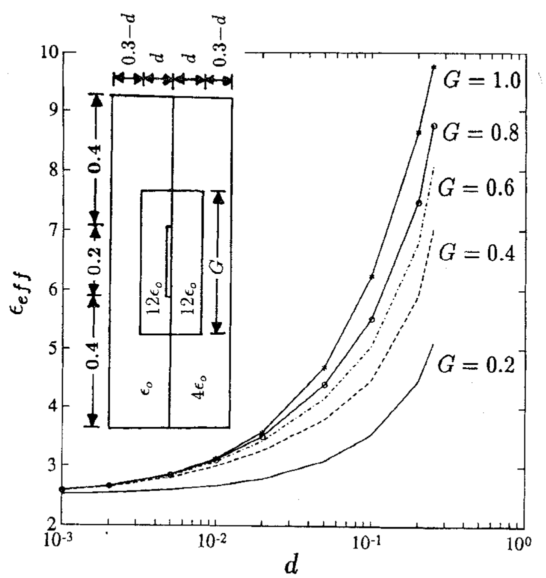

Fig. 5. Effective dielectric constant affected by the high permittivity enclosure.

line is shown as a function of lateral shift of the periodical substrate relative to the strip. In the substrate, the shaded areas represent glass fiber and the white areas represent epoxy. As more glass fiber is laterally shifted underneath the strip, the capacitance increases. The variation range is smaller for the structure with three interleaving layers. Because the mixture of epoxy in between fiber glass areas reduces the relative permittivity underneath the strip, thus the shift of substrate produces less significant permittivity change than the other configuration.

In Fig. 4, we present the effective dielectric constant of a microstrip line with an air pocket underneath the supproting film. The air pocket is observed to increase the phase velocity of the signal along the strip, and the effect is more significant with a larger pocket.

On the other hand, the phase velocity may be reduced by enclosing the strip with a high permittivity material. As shown in Fig. 5, the larger the area with high permittivity material, the slower the quasi-TEM signal will propagate. In both Figs. 4 and 5, the effective dielectric constant converges to that with a homogeneous substrate as d approaches zero.

Heat treatment is applied in certain applications when depositing micostrips onto the substrate, which may cause permittivity variation in the substrate right underneath the strip. In Fig. 6, we show the capacitance of two coupled microstrip lines with permittivity variation in the area underneath the strips. Both the self and mutual capacitance increase with

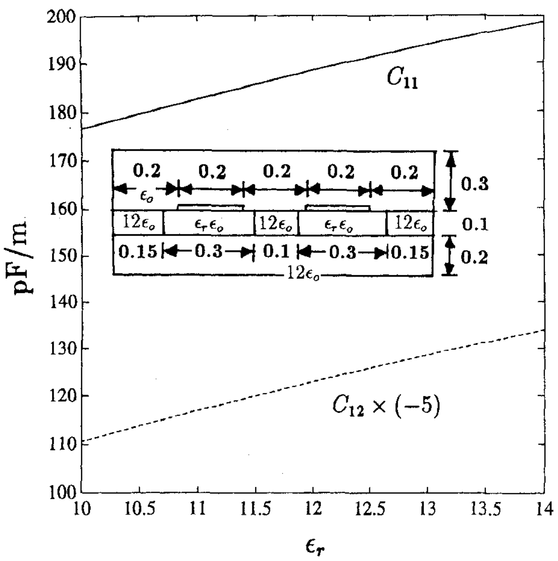

Fig. 6. Capacitance of coupled microstrip lines affected by the permittivity under the strips.

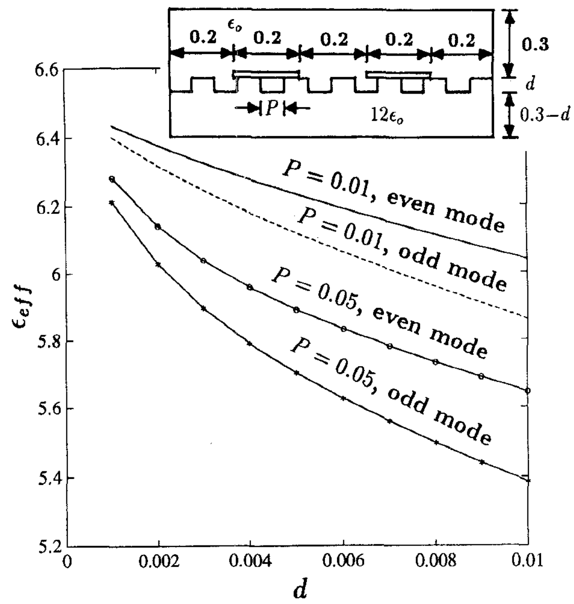

Fig. 7. Effective dielectric constant affected by the corrugated substrate surface.

increasing permittivity. The capacitances with $\epsilon_r = 12$ are those with a homogeneous substrate.

In Fig. 7, the effective dielectric constant of two coupled microstrip lines attached to a corrugated substrate surface is presented. The corrugation is used to model surface roughness. The effective dielectric constants of the even and the odd modes are defined as

$$\epsilon_{\text{eff}}^{(e)} = \frac{C_{11} + C_{12}}{C_{11}^0 + C_{12}^0}, \qquad \epsilon_{\text{eff}}^{(o)} = \frac{C_{11} - C_{12}}{C_{11}^0 - C_{12}^0}$$

where C_{11} and C_{12} are the self and mutual capacitance per unit length of two coupled strips embedded in inhomogeneous substrates, C_{11}^0 and C_{12}^0 are the self and mutual capacitance per unit length of the strips with all dielectrics replaced by free space.

The effective dielectric constant of the even mode is higher than that of the odd mode. Either increasing the corrugation depth d or period P reduces ϵ_{eff} because more free space is mixed with the substrate near the strips.

Next, consider protrusion or indentation of the substrate. In Fig. 8, both the self and mutual capacitances increase when the substrate is indented and the strip is plated at the bottom of the dent. In such case, the electric field tends to concentrate near the bottom of the configuration, which has a higher permittivity. When the strip is deposited on top of a protrusion, part of the electric field remains in the free space, and the capacitance decreases. The capacitances with $d = 0$ are those with a homogeneous substrate.

In Fig. 9, we show the effective dielectric constant of the odd mode for two coupled microstrip lines deposited on a film with an air pocket beneath. The phase velocity increases when the depth or width of the pocket is enlarged. Similar observations can be found with the even mode as shown in Fig. 10. In both figures, the effective dielectric constants tend to converge to those with a homogeneous substrate, but the

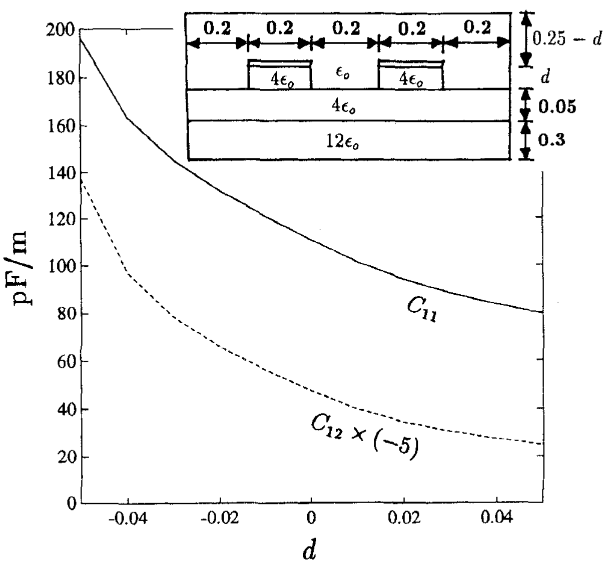

Fig. 8. Capacitance of coupled microstrip lines affected by the protrusion or indentation under the strips.

convergence is not as obvious as that for the single strip case shown in Figs. 4 and 5.

Finally in Figs. 11 and 12, we show the effective dielectric constants of two coupled microstrip lines with a high permittivity material under them. The effective dielectric constant increases as the depth or width of the high permittivity area is enlarged. The convergence to the effective dielectric constant with a homogeneous substrate is more obvious than that in Figs. 9 and 10.

All the results demonstrate that this technique can be applied to model microstrip lines with more complicated substrates such as with periodical loading of glass fibers (to enhance

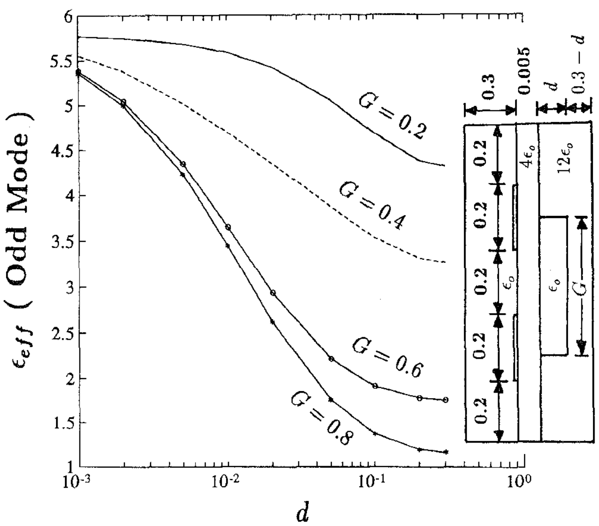

Fig. 9. Effective dielectric constant of coupled microstrip lines affected by the air pocket underneath the strips.

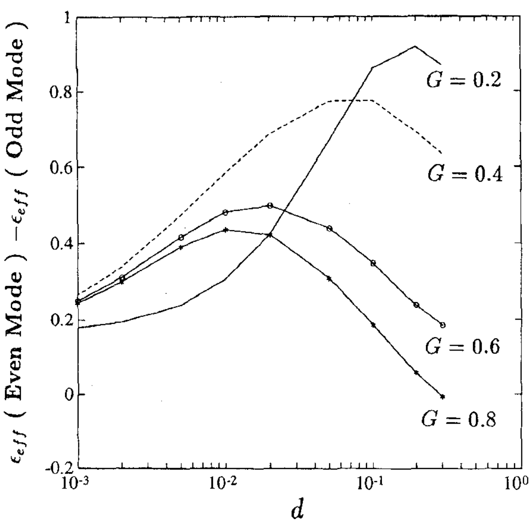

Fig. 10. Effective dielectric constant of coupled microstrip lines affected by the air pocket underneath the strips.

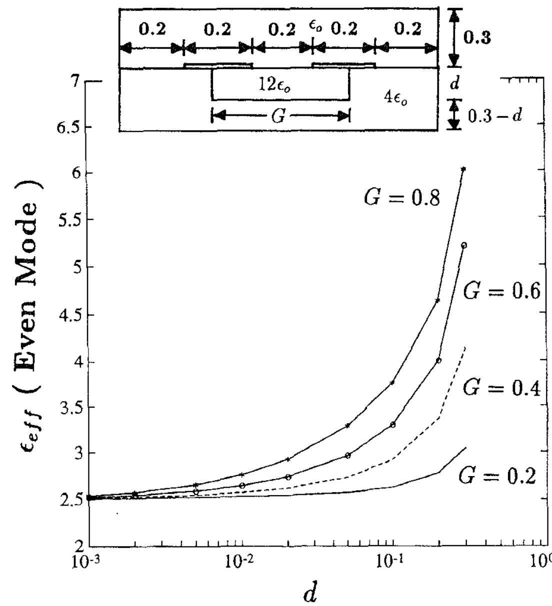

Fig. 11. Effective dielectric constant of coupled microstrip lines affected by the high permittivity zone in the substrate.

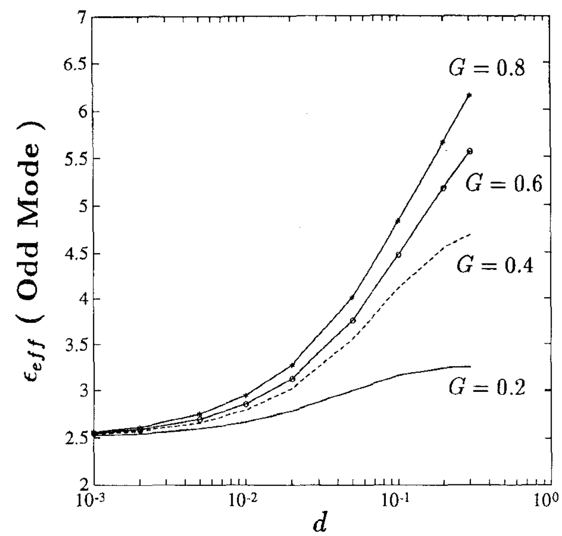

Fig. 12. Effective dielectric constant of coupled microstrip lines affected by the high permittivity zone in the substrate.

the substrate's mechanical strength), air pocket (to increase the phase velocity), high permittivity enclosure (to decrease the phase velocity), permittivity variation due to thermal treatment, surface roughness, protrusion or dent (to reduce or enhance coupling). Other structures occurring in applications with similar configuration can also be solved by using this technique.

IV. Conclusion

A mode-matching approach combined with Galerkin's method is proposed in this paper to calculate the capacitance matrix of microstrip lines embedded in an inhomogeneous stratified medium. The kernel of the integral equation is expressed in terms of eigenmodes solved numerically. Galerkin's method is applied to solve the charge distribution and hence the capacitance matrix. Several inhomogeneous dielectric profiles are studied to understand the effects of inhomogeneities on the capacitance and other related parameters like effective dielectric constant and phase velocity.

Acknowledgment

The author would like to thank the reviewers for their useful comments.

References

[1] D. Homentcovschi, "An analytical solution to the microstrip line problem," *IEEE Trans. Microwave Theory Tech.*, vol. 38, pp. 766–769, June 1990.

[2] D. Homentcovschi, A. Manolescu, A. M. Manolescu, and L. Kreindler, "An analytical solution for the coupled stripline-like microstrip line problem," *IEEE Trans. Microwave Theory Tech.*, vol. 36, pp. 1002–1007, June 1988.

[3] C. Wei, R. F. Harrington, J. R. Mautz, and T. K. Sarkar, "Multiconductor transmission lines in multilayered dielectric media," *IEEE Trans. Microwave Theory Tech.*, vol. MTT-32, pp. 439–450, Apr. 1984.

[4] S. M. Rao, T. K. Sarkar, and R. F. Harrington, "The electrostatic field of conducting bodies in multiple dielectric media," *IEEE Trans. Microwave Theory Tech.*, vol. MTT-32, pp. 1441–1448, Nov. 1984.

[5] J. Venkataraman, S. M. Rao, A. R. Djordjevic, T. K. Sarkar, and N. Yang, "Analysis of arbitrarily oriented microstrip transmission lines in arbitrarily shaped dielectric media over a finite ground plane," *IEEE Trans. Microwave Theory Tech.*, vol. MTT-33, pp. 952–959, Oct. 1985.

[6] E. Yamashita, "Variational method for the analysis of microstrip-like transmission lines," *IEEE Trans. Microwave Theory Tech.*, vol. MTT-16, pp. 529–535, Aug. 1968.

[7] S. Y. Poh, W. C. Chew, and J. A. Kong, "Approximate formulas for line capacitance and characteristic impedance of microstrip line," *IEEE Trans. Microwave Theory Tech.*, vol. MTT-29, pp. 135–142, Feb. 1981.

[8] F. Medina and M. Horno, "Capacitance and inductance matrices for multistrip structures in multilayered anisotropic dielectrics," *IEEE Trans. Microwave Theory Tech.*, vol. MTT-35, pp. 1002–1008, Nov. 1987.

[9] E. Drake, F. Medina, and M. Horno, "Quick computation of $[C]$ and $[L]$ matrices of generalized multiconductor coplanar waveguide transmission lines," *IEEE Trans. Microwave Theory Tech.*, vol. MTT-42, pp. 2328–2335, Dec. 1994.

[10] E. Pillai and W. Wiesbeck, "Derivation of equivalent circuits for multilayer printed circuit board discontinuities using full wave models," *IEEE Trans. Microwave Theory Tech.*, vol. 42, pp. 1774–1783, Sept. 1994.

[11] S. He, A. Z. Elsherbeni, and C. E. Smith, "Decoupling between two conductor microstrip transmission line," *IEEE Trans. Microwave Theory Tech.*, vol. 41, pp. 53–61, Jan. 1993.

[12] K. Wu, Y. Xu, and R. G. Bosisio, "A technique for efficient analysis of planar integrated microwave circuits including segmented layers and miniature topologies," *IEEE Trans. Microwave Theory Tech.*, vol. 42, pp. 826–833, May 1994.

[13] H. A. Haus and J. R. Melcher, *Electromagnetic Fields and Energy*. Englewood Cliffs, NJ: Prentice-Hall, 1989.

Jean-Fu Kiang (M'89) was born in Taipei, Taiwan, ROC, on February 2, 1957. He received the B.S.E.E. and M.S.E.E. degrees from National Taiwan University, and the Ph.D. degree from MIT, Cambridge, MA, in 1979, 1981, and 1989, respectively.

He was with IBM Watson Research Center, Bellcore, and Siemens. He is now with the Department of Electrical Engineering, National Chung-Hsing University, Taichung, Taiwan.